Correlation of microstructure and mechanical properties with ultrasonic velocity in the Ni-based superalloy Inconel 625

Article *in* Philosophical Magazine A · September 2002

DOI: 10.1080/01418610208240051

CITATIONS
40

READS
485

5 authors, including:

Anish Kumar
Indira Gandhi Centre for Atomic Research
169 PUBLICATIONS **1,791** CITATIONS
SEE PROFILE

Vani Shankar
Indira Gandhi Centre for Atomic Research
61 PUBLICATIONS **1,539** CITATIONS
SEE PROFILE

Kota bhanu sankara rao
University of Hyderabad
272 PUBLICATIONS **6,188** CITATIONS
SEE PROFILE

Baldev Raj
Indira Gandhi Centre for Atomic Research
919 PUBLICATIONS **18,400** CITATIONS
SEE PROFILE

Philosophical Magazine A, 2002, Vol 82, No. 13, 2529-2545

Correlation of microstructure and mechanical properties with ultrasonic velocity in the Ni-base superalloy Inconel 625

ANISH KUMAR, VANI SHANKAR, T. JAYAKUMAR, K. BHANU SANKARA RAO AND BALDEV RAJ

Metallurgy and Materials Group, Indira Gandhi Centre for Atomic Research
Kalpakkam 603102, India

ABSTRACT

Inconel 625 tubes are used extensively in ammonia cracker units of heavy water plants. During service, the alloy is exposed to temperature close to 873 K for prolonged period (~ 60,000 h) leading to substantial decrease in ductility and toughness of the alloy due to heavy intra and intergranular precipitation. Service exposed Inconel 625 material (873 K for ~ 60,000 h) was given post service ageing treatments at different temperatures (923 K, 1023 K and 1123 K) upto 500 h. These heat treatments altered the microstructure, which in turn had an influence upon both tensile properties and ultrasonic velocity. The service seen alloy was solution annealed at 1423 K for 0.5 h followed by ageing at different temperatures (923 K and 1123 K) and the influence of these heat treatments on changes in microstructures, and in turn their effect on room temperature tensile properties and ultrasonic velocity have been studied. The present study aims at establishing the correlation between room temperature tensile properties and ultrasonic velocity with the microstructural changes that occurred during ageing treatments in Ni-base superalloy Inconel 625. For the first time, authors' have brought out the influence of various precipitates, such as intermetallic phases γ", $Ni_2(Cr,Mo)$ and δ, and grain boundary carbides, on the correlation of yield strength and ultrasonic velocity.

§1. INTRODUCTION

Nickel base superalloy, Inconel 625 is currently used in aeronautical, aerospace, chemical petrochemical and marine applications. The choice for this material is based upon a good combination of its yield strength, tensile strength, creep strength, excellent fabricability, weldability and good resistance to high temperature corrosion on prolonged exposure in aggressive environments. Although the alloy was initially designed and used in solid solution strengthened condition, it is observed that precipitation of intermetallic phases and carbides occur on subjecting the alloy to ageing treatment in the range of 823 K to 1023 K (Eiselstein 1991). Precipitation hardening in this alloy at elevated temperatures (823 K-923 K) is mainly derived from the precipitation of metastable phase γ" [Ni_3(Nb, Al, Ti)] having ordered body-centered tetragonal DO_{22} structure and Ni_2(Cr, Mo) phase having orthorhombic Pt_2Mo type structure (Brown *et al.* 1991, Vani Shankar *et al.* 2001 and Sundararaman *et al.* 1999) The metastable γ" phase is transformed to the orthorhombic δ phase [Ni_3(Nb, Mo)] having DO_a structure upon prolonged aging (Brown *et al.* 1991 and Vani Shankar *et al.* 2001). The δ phase has also been reported to form directly from the supersaturated solid solution on ageing at higher temperatures (Vani Shankar *et al.* 2001). Precipitation of $M_{23}C_6$, M_6C and MC carbides occurs in the temperature range of 1033 K-1253 K (Muzyka *et al.* 1972). The occurrence of the carbides has also been reported upon service exposure at temperatures below 873 K (Sundararaman *et al.* 1999, Thomas *et al.* 1994 and Shah *et al.* 1999).

Inconel 625 tubes are used extensively in ammonia cracker units of heavy water plants. During service, the alloy is exposed to temperature close to 873 K for prolonged period

(~60,000 h) leading to substantial decrease in ductility and toughness of the alloy that subsequently leads to failure. Recently, degradation in the mechanical properties has been attributed to heavy precipitation of intermetallic γ" (Ni_3(Nb,Al,Ti)) and Ni_2(Cr, Mo) phases (Sundararaman *et al* 1999, Vani Shankar *et al.* 2001). The grain boundary has also been found to be decorated with continuous carbides after the service exposure (Sundararaman *et al.* 1999, Thomas *et al.* 1994 and Shah *et al.* 1999). The degraded mechanical properties of such a component can be regained to a significant extent by giving it a resolutionizing heat treatment. Some properties can even be regained by giving heat treatments in the intermediate temperature range. A few attempts have been made earlier in this direction (Sundararaman *et al.* 1999, Thomas *et al.* 1994, Shah *et al.* 1999). However, a thorough understanding is lacking even though a few time-temperature cycles of heat treatments are suggested for practical situations. For successful exploitation of regained mechanical properties, two conditions are essential, namely a reliable correlation between the microstructures and mechanical properties, and secondly a practical and accurate nondestructive technique for in-situ monitoring of the properties of Inconel 625 component, both during service and after post service heat treatment conditions. Nondestructive ultrasonic velocity measurements offer a good possibility to check for acceptance in nonuniformity of mechanical properties in the component.

Ultrasonic technique has been used extensively for characterization of microstructures, assessment of defects and evaluation of material properties. The use of ultrasonic measurements during fabrication and heat treatment ensures the absence of unacceptable discontinuities and presence of desired microstructure with acceptable properties (Shah *et al.* 1999). Ultrasonic in-service inspection is carried out to detect any unacceptable degradation in microstructure and formation and extension of defects during the operation of a component (Mignogma *et al.* 1980). Ultrasonic velocity measurements have been correlated with the microstructural features evolved during solutionizing (Anish Kumar and Laha *et al* 2000) and ageing (Anish Kumar and Choudhary *et al.* 2000) heat treatments in ferritic steels, superalloys (Jayakumar *et al.* 1991, 1997) aluminum alloys (Rosen *et al.,* 1985) and many other materials. In Nimonic alloy PE 16, Jayakumar et al. established correlations between the ultrasonic shear and longitudinal velocities and changes in density and elastic modulus resulting from the occurrence of secondary phases, such as γ' (Jayakumar *et al.* 1991, 1997). The velocity has also been shown to increase linearly with increase in the volume fraction of γ' precipitates in this alloy. However, in case of other complex superalloys, such as Inconel 718, Inconel 625 etc., in which more than one phase occurs, establishing a generalized correlation between ultrasonic velocity and mechanical properties is not possible. The ultrasonic velocity depends on the Young's modulus and density of the alloy, where as mechanical property, such as yield strength, depends on the degree of coherency, fineness and distribution of the precipitates. The synergistic influence of various precipitates on yield strength, Young's modulus and density (the later together influence the ultrasonic velocity) can be complex. Hence judicious selection of a combination of heat treatments are required to be planned meticulously to unfold the relative influence of each of the phases on yield strength and ultrasonic velocity for comprehensive understanding of the synergistic effect of different phases and utilization of the established correlation for practical applications. This is the objective of the study.

In the present study, correlations between ultrasonic velocity and yield stress have been established for various precipitates, such as different intermetallic phases (γ", Ni_2(Cr,Mo) and δ) and grain boundary carbides, by investigating the service exposed (SE) and post service heat treated Inconel 625 alloy. These correlations have been further confirmed for γ" and δ precipitates by investigation on solution annealed alloy aged at 923 K and 1123 K. The correlation for Ni_2(Cr,Mo) could not be confirmed as it has been reported to precipitate only

after very long exposure (≥ 40000 h) at temperatures below 873 K (Sundararaman *et al* 1999).

§2. EXPERIMENTAL DETAILS

2.1. Sample preparation

Bars of size 9 mm x 10 mm x 60 mm were machined from the SE Inconel 625 tube and the bars were then thermally aged at different temperatures (923 K, 1023 K and 1123 K) for different durations upto 500 h. The SE alloy was also resolutionized at 1423 K for 0.5 h and subsequently aged at 923 K and 1123 K upto 500 h. The chemical composition (in wt %) of the alloy investigated is as follows : Cr-21.7, Fe-3.9, Mo-8.8, Nb- 3.9, C- 0.05, Mn-0.14, Si-0.15, Al-0.17, Ti-0.23, Co-0.08 and Ni-balance. Microstructural characterization was carried out using optical microscope, Scanning Electron Microscope (SEM) and Transmission Electron Microscope (TEM). Specimens of 5mm thickness for optical microscopy were cut from one end of the heat treated bars. These were polished and etched etectrolytically for nearly 20 seconds using saturated oxalic acid solution at ~ 3-5 volts with a stainless steel cathode. Thin slices were cut from these samples and ground to a thickness of ~ 150 μm. Discs of 3 mm diameter were punched out and thinned using dual jet polishing technique in an electrolyte containing one part perchloric acid and four parts of ethanol at a temperature of ~ 230 K. Specimens, used for optical microscopy, were surface ground to obtain plane parallelism to an accuracy of ± 3 μm to enable precise ultrasonic velocity measurements.

2.2 Tensile testing

Standard tensile specimens of 4 mm diameter and 25 mm gauge length were machined and tested in air at room temperature (298 K) at a constant strain rate of 3.2×10^{-4} s^{-1}. Two specimens were tested for each microstructural condition. Yield stress and uniform percentage elongation were measured for these specimens.

2.3 Ultrasonic velocity measurements

The schematic for the experimental setup used for the ultrasonic measurements is given elsewhere (Anish Kumar et al 2002). Ultrasonic velocity was measured at room temperature using 15 MHz longitudinal wave and 5 MHz shear wave transducers. 100 MHz broad band pulser-receiver (M/s Accutron, USA) and 500 MHz digitizing oscilloscope (Tektronix TDS524) were used for carrying out the ultrasonic measurements. Cross correlation technique has been used for precise velocity measurements (Rao *et al.* 1993). The choice of the transducer frequency has been made keeping in view the normally used frequency range in practical applications. The ultrasonic velocity measurements were made at 500 MHz digitizing frequency and the gated backwall echoes from the oscilloscope were transferred to the personal computer with the help of GPIB interfacing and LabVIEW software. The accuracy in time of flight measurement was better than 1 ns and the maximum scatter in the ultrasonic longitudinal wave velocity (V_L) was ± 2.5 m/s for and ± 1.5 m/s for shear wave velocity (V_S). For calculating the Young's modulus (E) of the specimens by ultrasonic measurements, density measurements have been carried out for all the specimens using Archimedes principle. The accuracy for weight measurements was better than ± 0.0001 g. The liquid used for the density measurement was demineralized water. A set of at least three readings was taken for each specimen. The Young's modulus (E) has been calculated using the following equations (Ledbetter 1983 and Nondestructive Testing Handbok 1991):

$$E = V_L^2 \times \rho \times \frac{(1+\nu)(1-2\nu)}{(1-\nu)} \quad (1)$$

where ν is the Poisson's ratio defined as

$$\nu = \frac{(V_L^2 - 2 \times V_S^2)}{2 \times (V_L^2 - V_S^2)} \quad (2)$$

§3.0 RESULTS AND DISCUSSION

3.1 Microstructural Examination

Transmission Electron Microscopy carried out on SE alloy showed extensive intra and intergranular precipitation (Fig. 1a). Magnified image of Fig. 1a (Fig. 1b) showed that some of the intragranular precipitates were having snowflaky morphology (A in Fig. 1b) and others had lens shape (B in Fig. 1b). Figure 1c shows the selected area diffraction (SAD) patterns taken from the matrix using [001] zone axis. It can be seen from Figs. 1c and d that superlattice reflection occur at {100}, {110}, {1½0} and 1/3{220} positions. The {100}, {110} and {1½0} reflections arise from the γ" precipitate, where as 1/3{220} reflections arise from Ni_2(Cr, Mo) phase having Pt_2Mo type structure (Sundararaman *et al.* 1999). Further analysis revealed the lens shaped precipitates to be γ" (Ni_3(Nb, Al, Ti)) phase and the snow flake type precipitates to be Ni_2(Cr, Mo) phase. A continuous film of carbides at the grain boundaries could also be seen in Fig. 1a. Short duration aging at 923 K for 1 h led to the dissolution of the Ni_2(Cr,Mo) phase (Fig. 2a), which could be confirmed by the absence of 1/3{220} reflections corresponding to Ni_2(Cr,Mo) (Figs. 2b and c). Ageing the SE alloy to longer durations (500 h) at 923 K led to the precipitation of the δ (Ni_3(Nb, Mo)) phase in the form of elongated needles (Fig. 3). Ageing at intermediate temperature (1023 K) led to comparatively faster rate of dissolution of γ" along with Ni_2(Cr,Mo) precipitates. Precipitation of the δ phase occurred much earlier at 1023 K (after ≥10 h) than that at 923K (after ≥200 h). Ageing the SE alloy at 1123 K for 1 h led to the complete dissolution of both γ" and Ni_2(Cr,Mo) precipitates (Fig. 4a), which could be confirmed by the absence of the superlattice reflections corresponding to γ" and Ni_2(Cr,Mo) phases in the SAD taken from the matrix (Fig. 4b and c). Ageing for longer duration at 1123 K led to the precipitation of the δ phase (Fig. 5a), the volume fraction of which increased with ageing time (Figs. 5b and c). Carbides were observed at the grain boundaries during all the temperatures of treatments employed to the SE alloy.

The resolution annealing of the alloy at 1423 K for 0.5 h dissolved the grain boundary carbides also along with all the intermetallic precipitates without affecting the grain size (Fig. 6a). Further ageing at 923 K and 1123 K led to the precipitation of intermetallic phases γ" (Fig. 7a) and δ respectively along with the precipitation of secondary carbides.

3.2 Mechanical Properties

Figures 8a and b show respectively the variation in yield stress (YS) and percentage uniform elongation with ageing time for the SE and resolution annealed (RSA) alloy. It was observed from Figs. 8a and b that the SE alloy had a very high YS value of ~ 1013 MPa and a low elongation of ~ 6% as compared to YS of ~ 375 MPa and elongation of ~ 60 %, prior to putting the alloy in service i.e. in solution annealed condition. The high yield strength of the SE alloy is attributed to the precipitation hardening derived from the intragranular γ" and Ni_2(Cr, Mo) precipitates. Subjecting the SE alloy to temperatures higher than the service

temperature, led to a decrease in the YS value and a corresponding increase in the ductility due to the dissolution of these precipitates. The extent of reduction in the YS value of the SE alloy increased with the increase in the ageing temperature and / or duration of ageing. The largest decrease in the YS value (600 MPa decrease) during 1 h ageing at 1123 K resulted from the complete dissolution of both the intermetallic phases. Comparatively smaller decrease in YS (170 MPa decrease) at 923 K was due to the dissolution of only the Ni_2(Cr, Mo) phase. Dissolution of Ni_2(Cr,Mo) phase had more influence upon the yield strength as compared to that on ductility. This is in agreement with the observations made in other Ni-base superalloys (Tawancy 1980).Ageing at 1023 K exhibited the intermediate behavior. Ageing beyond 1h at 1123 K, increased the YS and decreased the elongation due to the precipitation of δ phase as discussed earlier.

The resolution annealing at 1423 K for 0.5 h decreased the yield stress to 370 MPa (40 MPa less than that for the specimen heat treated at 1123 K for 1 h having only grain boundary carbides) as shown in Fig. 8a and increased the ductility to 58 % elongation (5 % more that that for the specimen heat treated at 1123 K for 1h) as shown in Fig. 8b. Ageing the RSA alloy at 923 K increased the yield stress to a higher value (770 MPa after 500 h of ageing, Fig. 8a) as compared to that at 1123 K (455 MPa after 500 h of ageing, Fig. 8a), whereas the ductility was found to decrease more at 1123 K (20 % total elongation after 500 h of ageing, Fig. 8b) as compared to that at 923 K (29 % total elongation after 500 h of ageing, Fig. 8b).

The above results clearly indicate that the room temperature mechanical properties of Inconel 625 are predominantly affected by the intermetallics and to a lesser extent by the grain boundary carbides. The effect of γ" precipitate on YS was found to be more pronounced than that of δ precipitate and the ductility was found to be affected more by δ precipitate than the γ" precipitate.

3.3 Ultrasonic Velocity measurements

Figure 9a shows the variation in ultrasonic longitudinal wave velocity with ageing time for SE and RSA specimens. Ultrasonic velocity was found to be highest (5904 m/s) in the SE condition due to the presence of intermetallic precipitates. The intermetallic precipitates have been reported to increase the elastic moduli of the alloy and hence the ultrasonic velocities in superalloys (Jayakumar *et al.* 1991, 1997 and Fisher 1986). Ageing for shorter durations at all the temperatures decreased the ultrasonic velocity due to dissolution of the intermetallic precipitates. The dependence of YS and ultrasonic velocity on ageing temperature and time exhibited the similar behaviour. Ultrasonic velocity was found to increase with the precipitation of δ phase. Ageing the SE specimen at 923 K decreased the ultrasonic velocity from 5904 m/s to 5852 m/s (52 m/s decrease from SE specimen), which is attributed to the dissolution of Ni_2(Cr,Mo) precipitates. Ultrasonic velocity decreased to 5832 m/s (i.e. 72 m/s from SE specimen) upon ageing at 1123 K for 1 h due to dissolution of both Ni_2(Cr,Mo) and γ" precipitates. Beyond one hour of ageing, it increased monotonously due to the precipitation of δ phase (Fig. 9a). The difference in the minimum velocity at 923 K and 1123 K (22 m/s) is attributed to the dissolution of γ" precipitates. Even after the resolution annealing, the ultrasonic velocity was found to be almost similar to that after 1h ageing at 1123 K as shown in Fig. 9a. This showed that ultrasonic velocity is only affected by the intermetallic precipitates and not by the grain boundary carbides. Ageing the RSA alloy at both the temperatures, 923 K and 1123 K, increased the ultrasonic velocity as shown in Fig. 9a, but the increase was found to be more drastic at 1123 K (5864 m/s after 500 h) with the precipitation of δ phase as compared to that at 923 K (5854 m/s after 500 h) where γ" was found to precipitate.

Variation in Young's modulus with post service ageing time also exhibited similar behaviour as that of ultrasonic velocity (Fig. 9b), indicating that the change in ultrasonic velocity in Inconel 625 is predominantly associated with the change in Young's modulus, rather than density changes, due to the formation and dissolution of various precipitates. Young's modulus was found to be highest in the SE specimen (~213 GPa) and lowest in the RSA alloy (~201 GPa), i.e. the exposure to temperature close to 873 K for prolonged period (~ 60,000 h) during service increased the Young's modulus of the alloy by 12 GPa (6 %) due to the precipitation of intermetallic phases.

Figure 10 shows the variation in yield stress with ultrasonic velocity for different heat treated specimens. To study the effect of different precipitates on extent of changes in YS and ultrasonic velocity, the total changes (from SE alloy to RSA alloy) are normalized to 100 % for both the YS and ultrasonic velocity. The changes for different heat treated conditions are calculated with respect to the SE conditions and are normalized to the total change from SE alloy to RSA alloy, as shown in Eqs. 3 and 4.

$$\% \text{ of total change in velocity } (\% \Delta V_x) = (V_x - V_{SE}) / (V_{SE} - V_{RSA}) \quad (3)$$

$$\% \text{ of total change in yield stress } (\% \Delta YS_x) = (YS_x - YS_{SE}) / (YS_{SE} - YS_{RSA}) \quad (4)$$

where V_x and YS_x are ultrasonic velocity and YS for any particular microstructural condition for which the change in velocity/YS ($\% \Delta V_x / \% \Delta YS_x$) is being calculated and V_{SE} ,V_{RSA} , YS_{SE} and YS_{RSA} are the ultrasonic velocity and YS in SE and RSA alloy respectively. The change for SE condition comes to 0 % (O in Fig. 10) and for RSA condition, it comes to -100 % (F in Fig. 10). It can be seen from Fig. 10 and Table 1 that during ageing the SE alloy at 923 K, 80 % change in ultrasonic velocity is associated with only 30 % change in YS (OA in Fig. 10), whereas, at 1023 K and 1123 K the 90 % and 100 % change in ultrasonic velocity are associated with 60 % (OB in Fig. 10) and 95 % (OD in Fig. 10) change in YS respectively. These results indicate that the effect of dissolution of only Ni_2(Mo, Cr) precipitates that takes place at 923 K, is more pronounced on ultrasonic velocity as compared to that on YS. In comparison to the YS, the velocity is less affected by the presence of γ" precipitates. Further, it can be seen in Fig. 10 that during the precipitation of δ phase at 1023 K (transformation of γ") ultrasonic velocity increases but YS is not affected much (BC in Fig. 10), whereas at 1123 K (direct precipitation of δ-phase), both the ultrasonic velocity and YS increase but the increase in ultrasonic velocity is 40 % whereas the increase in YS is only 20 % (DE in Fig. 10). This also confirms the earlier observation that the effect of γ" is more on YS as compared to the ultrasonic velocity and the effect of δ-phase is more on ultrasonic velocity as compared to the YS. This could be further confirmed by the ageing study carried out on the resolutionized alloy. It can be seen from Fig. 10 that during the precipitation of γ" phase at 923 K (FH in Fig. 10), the slope of the plot is much less as compared to that during the precipitation of δ phase at 1123 K (FG in Fig. 10). The influence of direct precipitation of δ phase on YS and velocity during the ageing of the SE alloy and resolutionized alloy has found to show similar behaviour (i.e. the same slopes for FG and DE in Fig. 10).

It can be seen from Fig. 10, that ultrasonic velocity and YS can be correlated linearly for different precipitates, as in equation 1.

$$YS = YS_0 + m\,(V - V_0) \quad (5)$$

Where, YS_0, V_0, YS and V are initial yield stress, initial ultrasonic velocity, yield stress in presence of precipitates and ultrasonic velocity in presence of precipitates respectively and m is a constant (slope). Table-1 also shows the values of slope (m) of equation-5 for

precipitation and dissolution of various precipitates. The slopes of equation-5 for the dissolution of Ni_2(Cr,Mo) phase (3.83) and precipitation of δ-phase (4.5) are much less as compared to that for the dissolution of the γ" precipitate (18.3) from the SE alloy. The above correlations could be further confirmed by investigation on the alloy solution annealed and aged at 923 K and 1123 K. The slope of equation-5 for the precipitation of δ and γ" phases from RSA alloy are found to be 3.1 and 17.4 respectively. These values are very close to that obtained for dissolution and precipitation of similar phases from SE alloy and this further confirms the earlier observation that the effect of γ" is more on YS as compared to the ultrasonic velocity and the effects of Ni_2(Cr,Mo) and δ phases are more on ultrasonic velocity as compared to the YS.

The dependencies of various individual precipitates on the correlation between YS and ultrasonic velocity, as presented in Fig. 10, have been derived from different ageing conditions employed to different starting conditions (SE or RSA). In fact, the effect of any particular type of precipitate is derived from specific heat treatments given in such a way that only that particular type of precipitate is affected, such as 1123 K treatment to RSA alloy and SE alloy after 1h treatment led to the precipitation of only δ phase and hence its effect could be studied clearly. Similarly 923 K treatment to SE alloy upto 200 h led to the dissolution of only the Ni_2(Cr,Mo) type of precipitate and its effect could also be studied clearly. However, 1023 K treatment led to the changes in γ″ phase also along with the dissolution of Ni_2(Cr,Mo) phase. Hence the changes occurring at this temperature have not been taken for the estimation of any correlation. The effect of γ″ phase on the correlation of YS and ultrasonic velocity has been estimated from SE alloy by comparing the SE alloy aged at 923 K for 200 h (containing grain boundary carbides and γ″ phase) and at 1123 K for 1 h (containing only grain boundary carbides). This correlation was also confirmed by the precipitation of γ″ phase upon ageing the RSA alloy at 923 K.

The above mentioned correlation has practical significance in the monitoring of mechanical properties degradation during the service, i.e. if the type of precipitate that forms is known a priori (based on the service temperature and time durations), proper correlation of ultrasonic velocity and yield strength can be used to assess the yield strength nondestructively by measuring the ultrasonic velocity.

The study points out that the rejuvenation of mechanical properties by post service heat treatments can be ensured by specifying a minimum ultrasonic velocity (~5830 m/s) after post service treatment, as a quality control parameter. The change in ultrasonic velocity during service can also be used to monitor the microstructural condition of the alloy and hence the extent of degradation in mechanical properties. The variation in the thickness of the actual component can be taken care of by carrying out the ultrasonic velocity measurements at the same place during service or by using the ratio of ultrasonic longitudinal and shear wave velocities, if feasible.

§4. Conclusion

The present study revealed that the long term exposure of Inconel 625 at temperature close to 823 K leads to the precipitation of intermetallic phases, γ" and Ni_2(Cr, Mo) which increases the yield stress of the material and decreases the ductility. The loss in ductility in the SE material can be partially regained by ageing for shorter durations at temperatures above service temperature. Ageing at 923 K has been found to be sufficient to dissolve the Ni_2(Cr, Mo) phase, whereas ageing at 1123 K dissolves both types of intermetallic precipitates, γ" and Ni_2(Cr, Mo). Ageing for longer duration results in the precipitation of undesirable δ-phase, which increases the yield stress and decreases the ductility. It is necessary to ensure that a proper time and temperature combination is employed to regain the

mechanical properties. Change in microstructure and mechanical properties during rejuvenation of degraded properties by post service heat treatments can be monitored nondestructively by using ultrasonic velocity measurements and by specifying a minimum ultrasonic velocity (~5830 m/s) as a quality control parameter for post service heat treated alloy.

The present study also shows the feasibility of monitoring the degradation in mechanical properties during the service using ultrasonic velocity measurements.

For the first time, the authors have brought out the synergistic influence of various precipitates, such as intermetallic phases (γ", $Ni_2(Cr,Mo)$ and δ) and grain boundary carbides, on correlation between yield stress and ultrasonic velocity. The study revealed that the room temperature tensile properties, i.e. YS and ductility, are dominantly affected by the intermetallic precipitates and less by the grain boundary carbides, where as ultrasonic velocity is only affected by the intermetallic precipitates and not by the grain boundary carbides. It has also been observed that the dissolution of $Ni_2(Cr, Mo)$ phase and precipitation of δ-phase have more effect on ultrasonic velocity as compared to that on yield stress, whereas dissolution and precipitation of γ" has more influence on yield stress than on ultrasonic velocity. This has practical significance in the monitoring of mechanical properties degradation during the service. This study has demonstrated that ultrasonic velocity measurements can be used in a deterministic way for the assessment of monitoring the degradation in mechanical properties during service and also for rejuvenation of the degraded mechanical properties during post service heat treatments.

ACKNOWLEDGMENTS

We are thankful to Prof. K. K. Ray for useful discussions. We are also thankful to Dr. S.L.Mannan, Associate Director, MDG and Mr. P.Kalyanasundaram, Head, DPEND for their cooperation.

REFERENCES

Anish Kumar, Laha, K., Jayakumar, T., Rao, K. Bhanu Sankara and Baldev Raj, 2000, "Comprehensive microstructural characterization in modified 9Cr-1Mo ferritic steel using ultrasonic measurements", 2002, *Metall. and Mater. Trans.*, In Press.

Anish Kumar, Choudhary, B.K., Jayakumar, T., Rao, K. Bhanu Sankara and Baldev Raj, 2000, *Trans. Indian Institute of Metals*, **53 (3)**, 341.

Brown, E.E. and Muzyka , D.R., 1987, *The Superalloys II*, C.T. Sims and W.C. Hagel, eds., John Wiley, New York, NY, 165.

Eiselstein, H.L. and Tillack, D.J. 1991, *Superalloy 718, 625 and Various Derivatives*, E.A. Loria, ed., TMS, Warrendale, PA, 1.

Fisher, E.S., 1986, *Scripta Mater.*, **20,** 279.

Jayakumar, T., Baldev Raj, Willems, H. and Arnold, W., 1991, *Review of Progress in Quantitative, NDE*, Plenum Press, New York., **10b**, 1693.

Jayakumar, T., 1997, Microstructural characterization in metallic materials using ultrasonic and magnetic methods, Ph. D. Thesis, University of Saarland, Saarbruecken, Germany.

Ledbetter, H. M., 1983, *Materials at low temperatures*, Edt. Reed, R.P. and Clark, A.F., American Soc. for Metals, Metals Park, Ohio 44073, 1.

Mignogma, R. B., Duke, J. C. Jr. and Green, 1980, *Materials Evaluation*, **38,** 37.

Muzyka, D. R., *The Superalloys*, 1972, Ed. C. T. Sims & W. C. Hagel, John Wiley, New York, pp. 113.

NDT Handbook, Second edition, 1991, *Ultrasonic Testing*, Edt. P Mclntire, Americal Society for Nondestructive Testing, USA, **7**, 836.

Papadakis, E.P., 1970, *Met. Trans.*, **1**, 1053-1057.

Rao, B. P. C., Jayakumar, T., Bhattacharya, D. K. and Baldev Raj, 1993, *J. Pure and Appl. Ultrasonics*, **25**, 53.

Rosen, M., Ives, L., Ridder, S., Biancaniello, F. and Mehrabian, R., 1985, *Mat. Sci. Engg.*, **74,** 1.

Shah, B.K., Nanekar, P.P., Bandyopadhyay, M., Bandyopadhyay, A.K., Biswas, A.K. and Kulkarni, P.G., 1996, *14th World Conference on Non Destructive Testing(14th WCNDT)*, New Delhi, India, 2235.

Shah, B.K., Anish Kumar, Bandyopadhyay, M., Bandyopadhyay, A.K. and Kulkarni, P.G., 1999, *INSIGHT*, **41 (11)**, 707.

Sundararaman, M., Lalit Kumar, Prasad, G.E., Mukhopadhyay, P. and Banerjee S., 1999, *Met. and Mater. Trans. A*, **30A**, 41.

Tawancy, H.W., 1980, *Metall. Trans. A*, **11A,** 1764.

Thomas, C. and Tait, P., 1994, *Int. J. Pressure Vessels Piping*, **59**, 41.

Vani Shankar, Rao, K. Bhanu Sankara and Mannan, S.L., 2001, *J. Nuclear Materials*, **288 (2-3)**, 222.

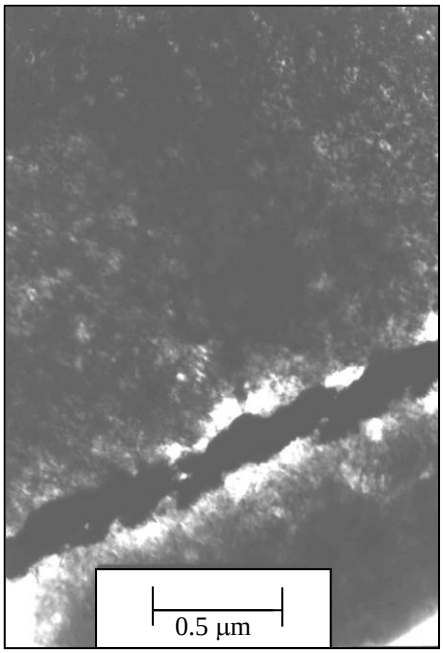

(a)

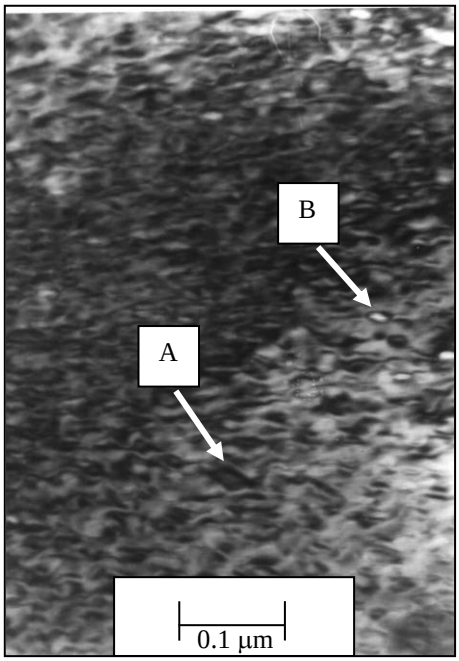

(b)

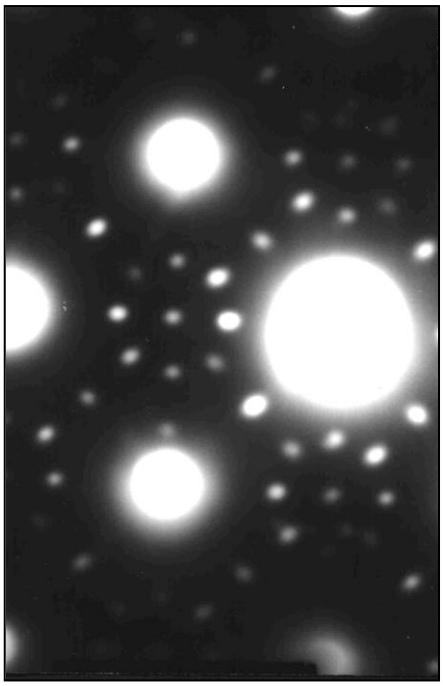

(c)

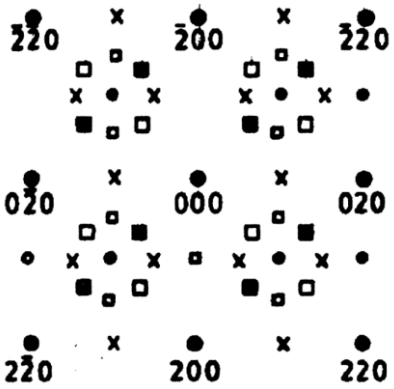

(d)

Fig. 1 (a) BF image of service-exposed alloy showing extensive intragranular precipitation and grain boundary carbides (b) Magnified image of (a) showing snowflaky (A) and lens (B) morphology of Ni_2 (Cr, Mo) and γ″ phases respectively (c) SAD taken from matrix using [001] zone axis showing superlattice reflections of both Ni_2 (Cr, Mo) and γ″ precipitates. (d) Key to diffraction pattern shown in (c), in this pattern □ and ■ represent the two variants of the Ni_2 (Cr, Mo) phase and ×, • and ▫ represent the superlattice reflections corresponding to the [100], [010] and [001] variants of γ″ phase.

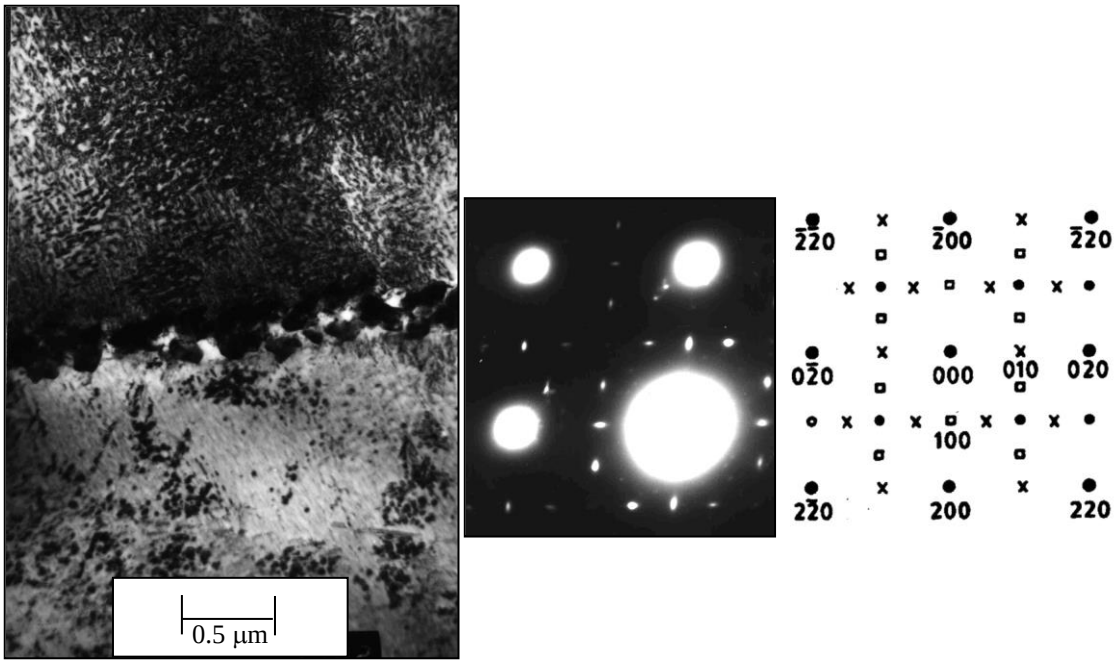

(a) (b) (c)

Fig. 2 (a) BF image of service-exposed alloy aged for 1h at 923 K, showing mainly γ″ and intergranular carbides (b) SAD taken from the matrix shows strong γ″ superlattice reflections (c) Key to diffraction pattern shown in (b), in this pattern ×, • and ▫ correspond to the three variants of γ″ phase.

Fig. 3. SEM micrograph of service-exposed alloy aged at 923 K for 500h showing elongated precipitates of δ.

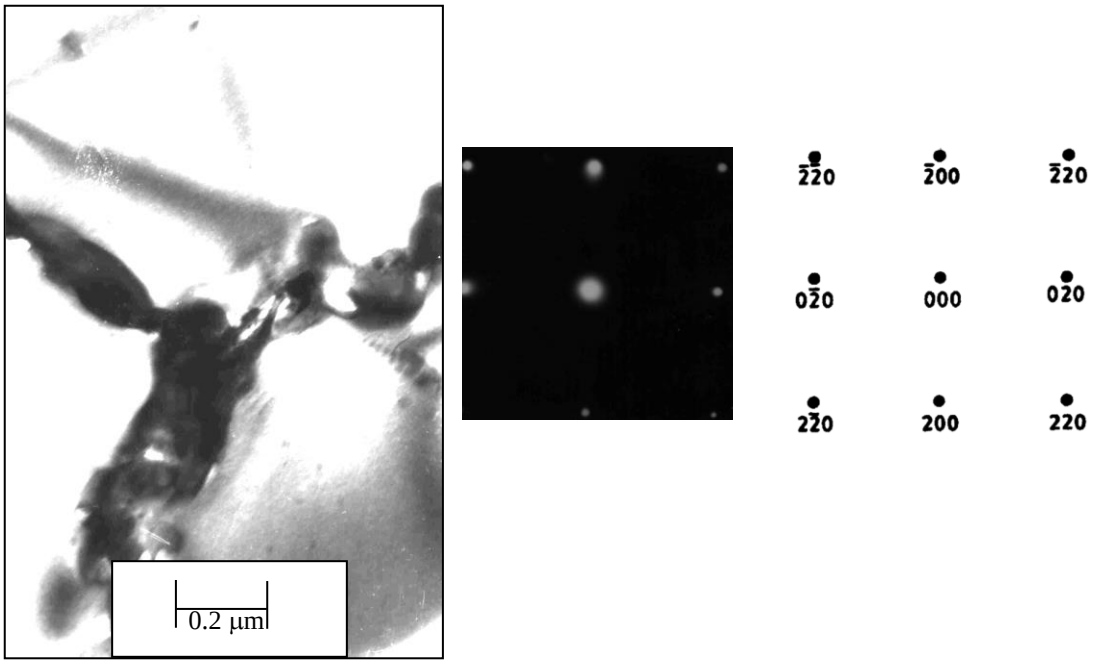

(a) (b) (c)

Fig. 4. (a) BF image of service exposed alloy aged for 1h at 1123 K, showing intergranular carbides only (b) SAD taken from the matrix showing the absence of Ni_2 (Cr, Mo) and γ'' phases (c) Key to diffraction pattern shown in (b).

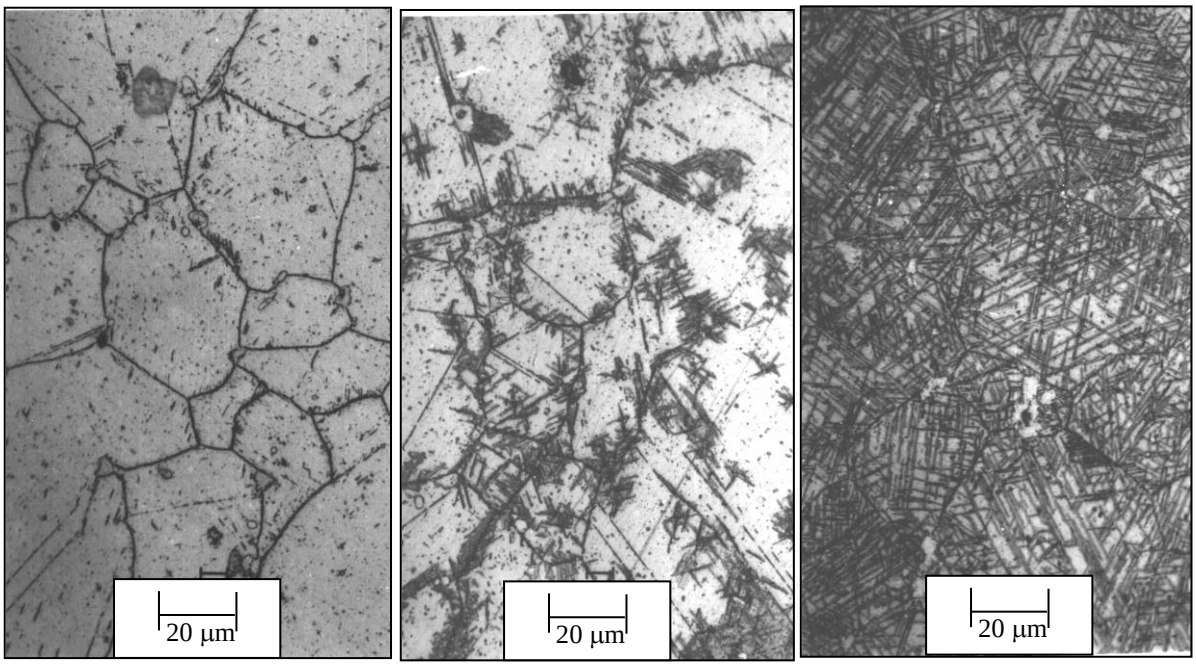

(a) (b) (c)

Fig. 5. Optical micrographs of the service exposed alloy aged at 1123 K for (a) 10 h (b) 100 h and (c) 500 h depicts increase in volume fraction of δ precipitate with ageing time.

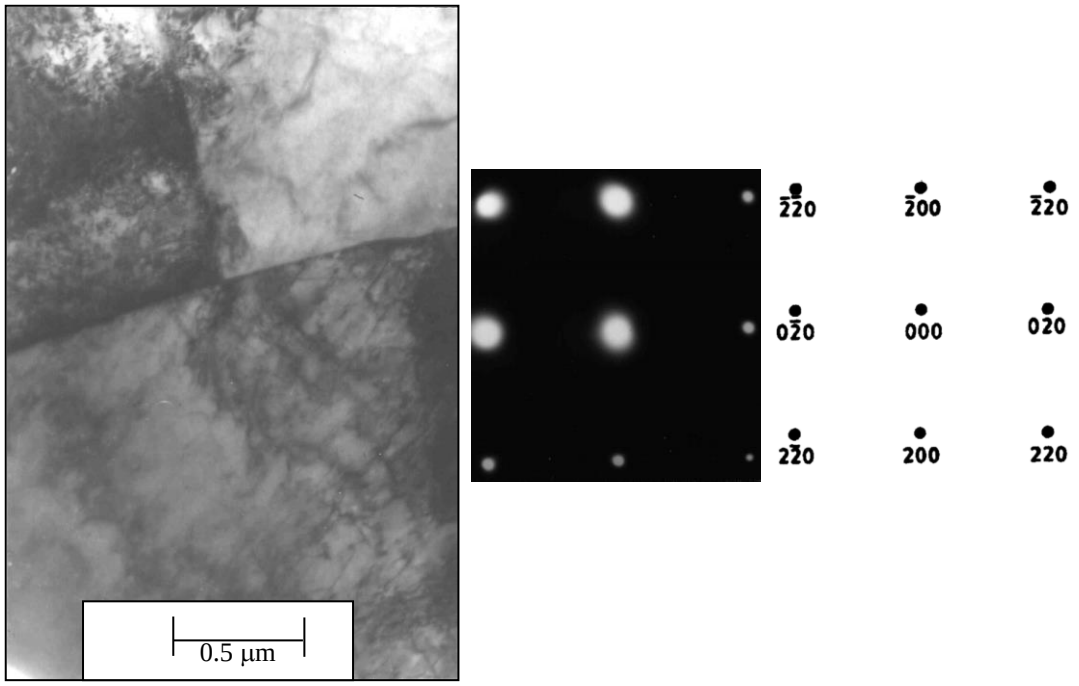

(a) (b) (c)

Fig. 6. (a) BF image of service-exposed alloy re-solution annealed at 1423 K for 0.5h showing quenched in dislocations, (b) SAD taken from matrix using [001] zone axis and (c) Key to diffraction pattern shown in (b).

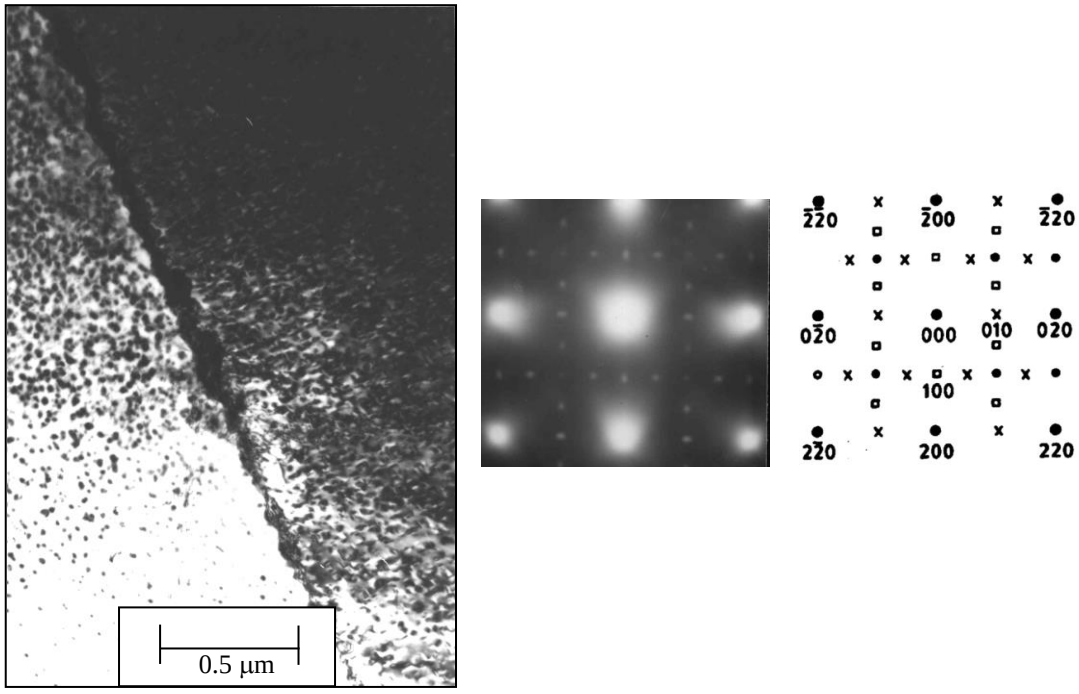

(a) (b) (c)

Fig. 7. Re-solution annealed alloy aged at (a) 923 K for 100h showing grain boundary carbides and γ″ (b) SAD taken from the matrix showing γ″ superlattice reflections (c) Key to diffraction pattern shown in (b), in this pattern ×, ▫ and • correspond to the three variants of γ″ phase.

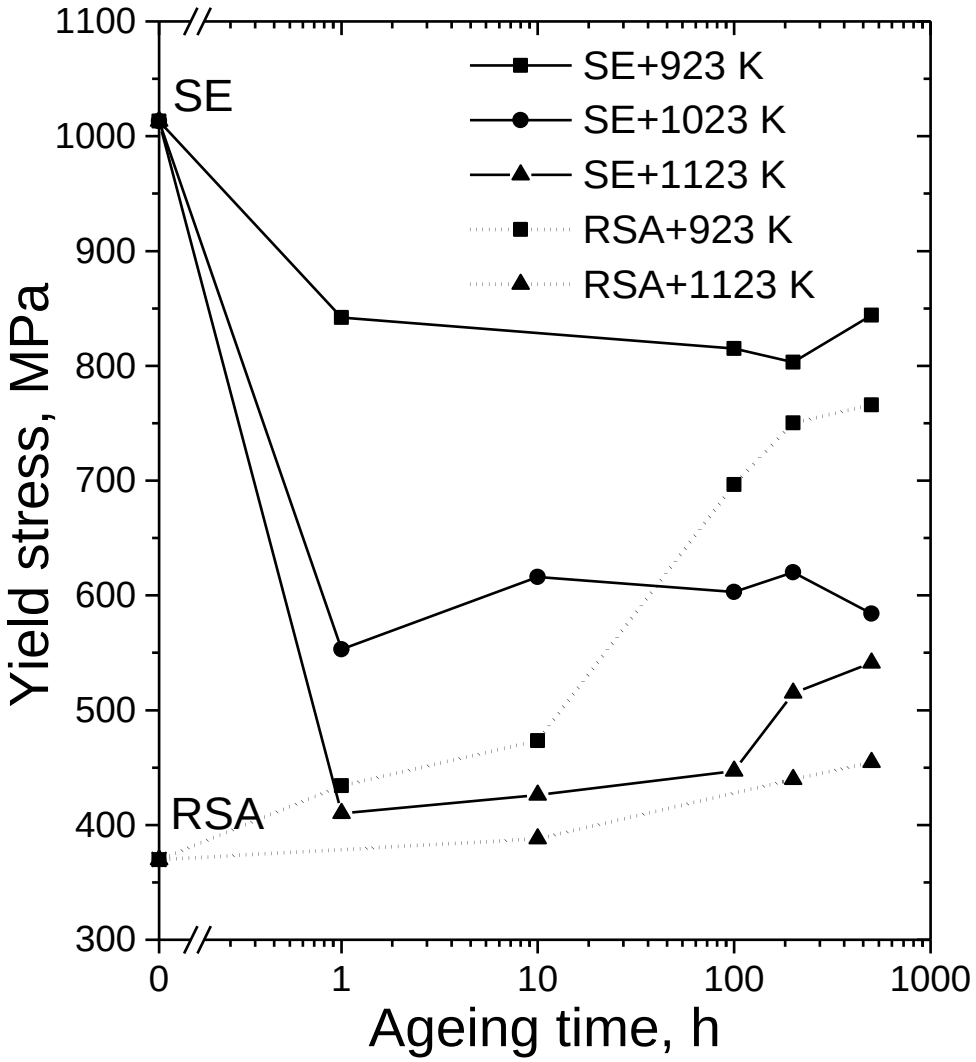

Fig. 8a. Variation in yield stress with ageing time for service exposed (SE) and resolution annealed (RSA)alloy.

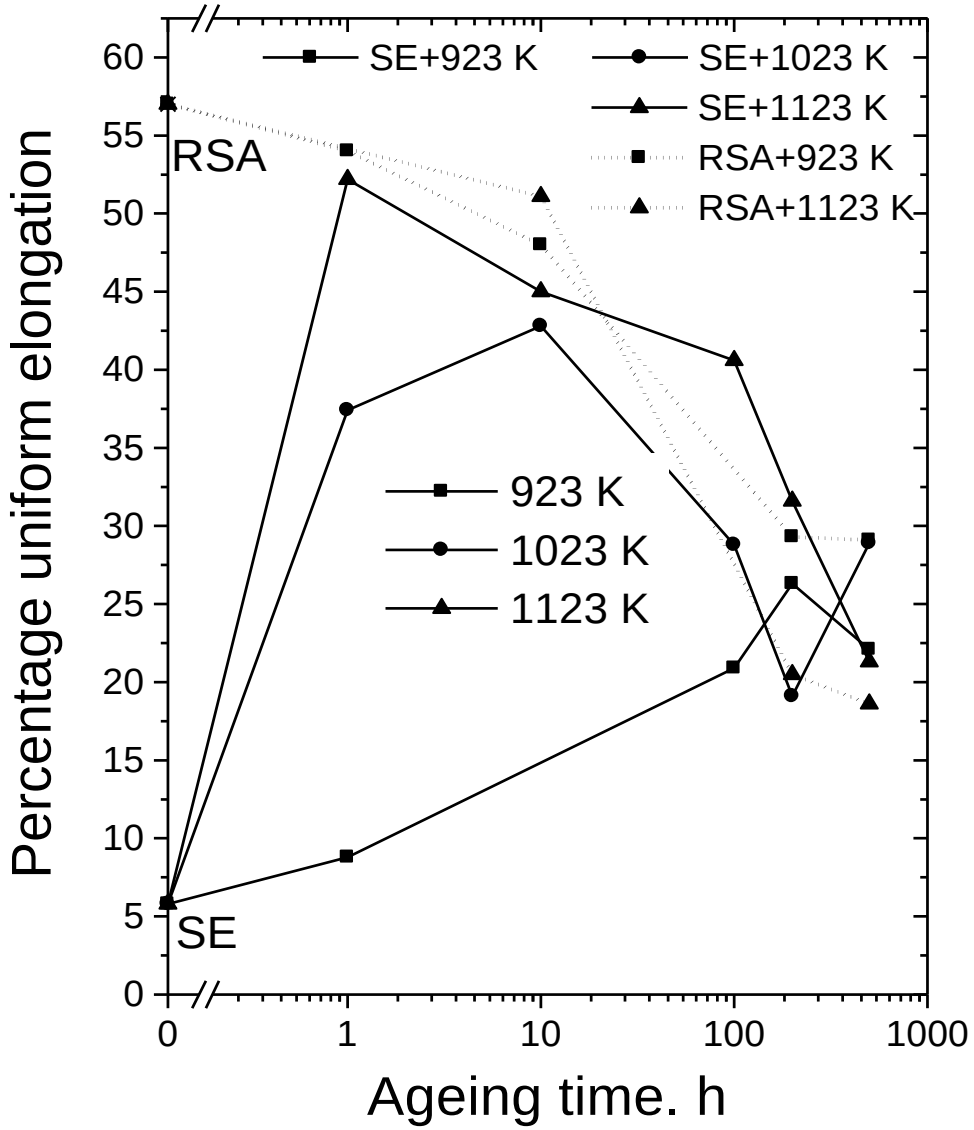

Fig. 8b. Variation in uniform percentage elongation with ageing time for service exposed (SE) and resolution annealed (RSA) alloy.

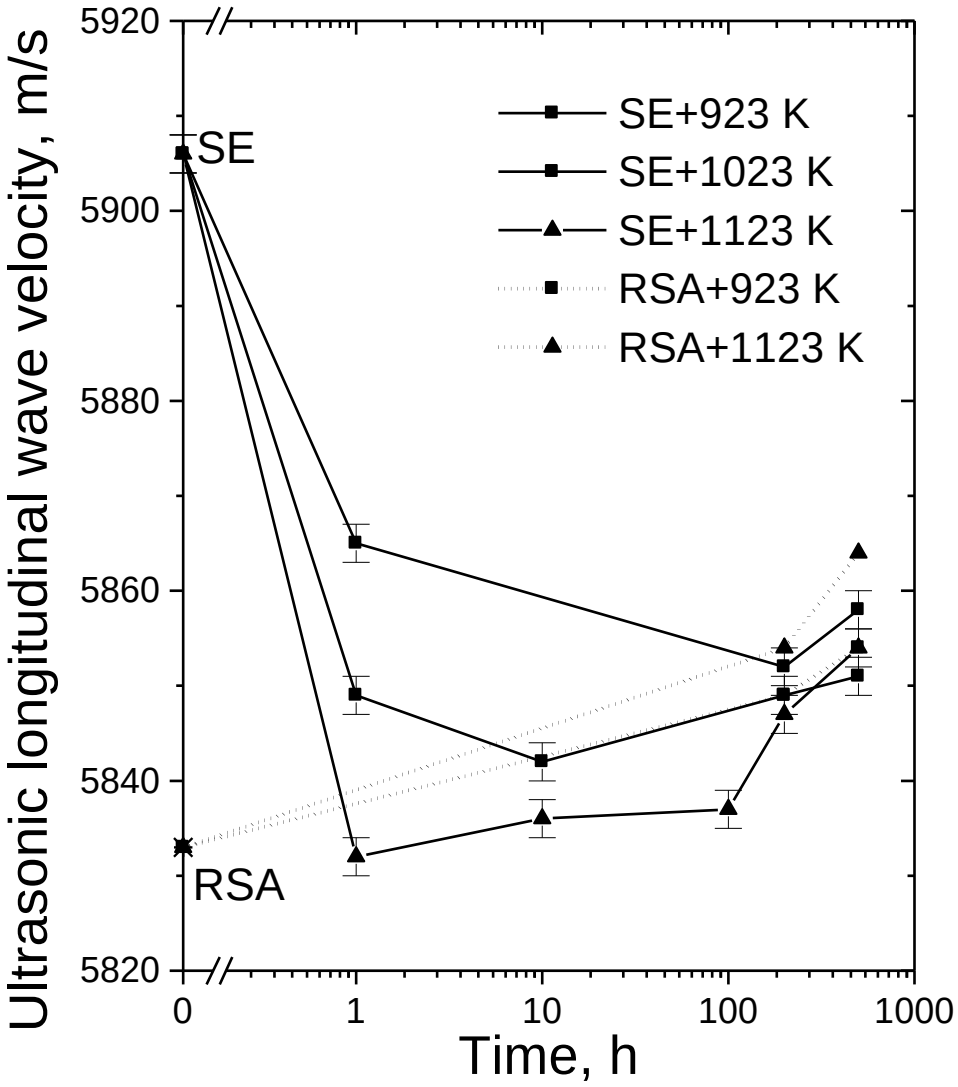

Fig. 9a. Variation in ultrasonic velocity with ageing time for service exposed (SE) and resolution annealed (RSA)alloy.

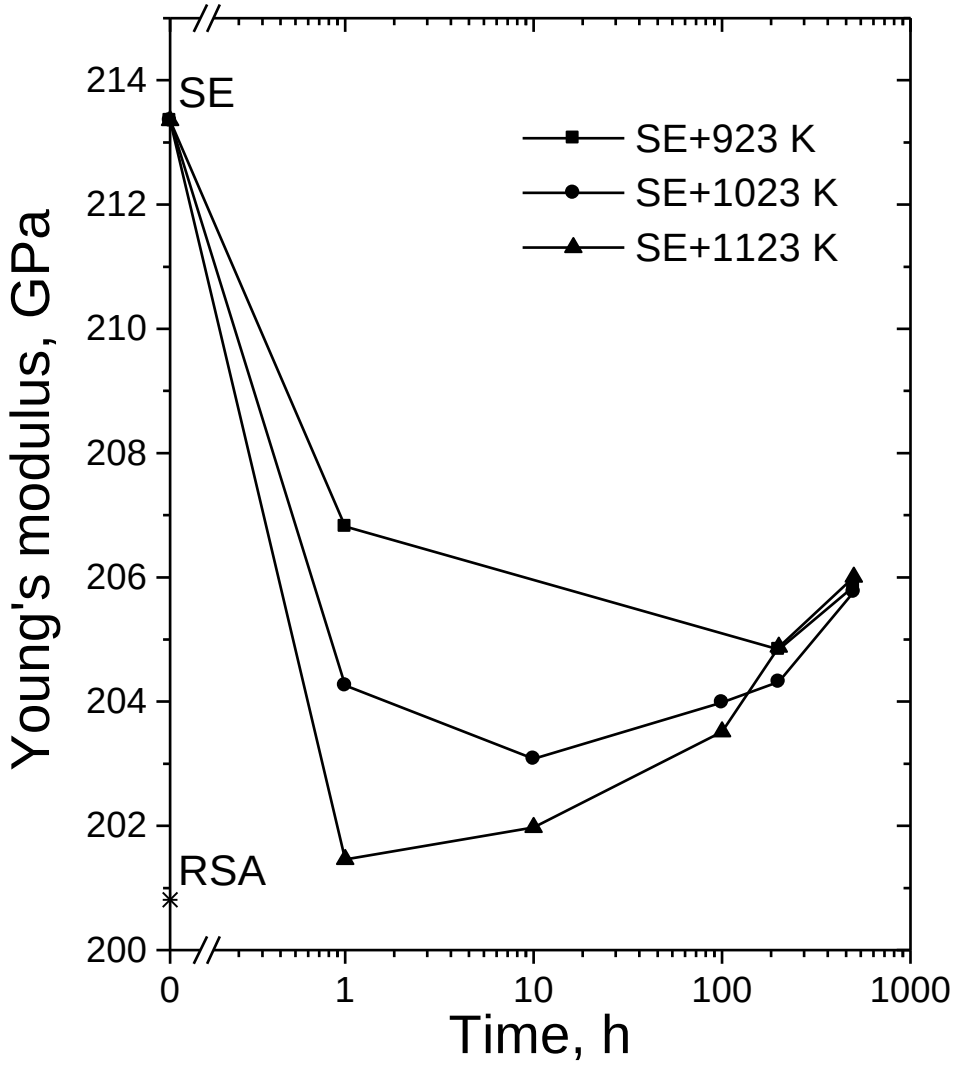

Fig. 9b. Variation in Young's modulus with post service ageing time.

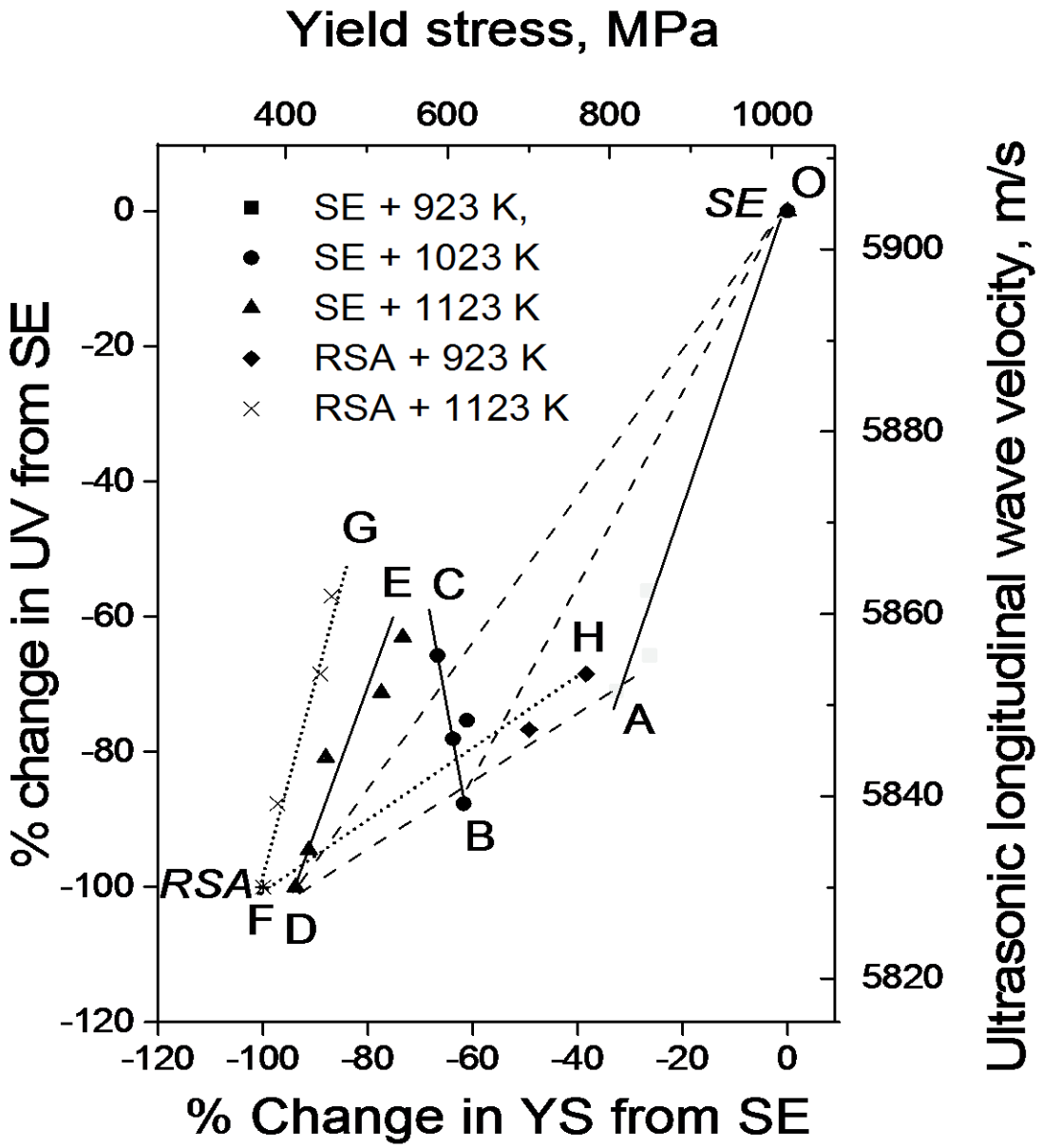

Fig. 10. Variation in ultrasonic longitudinal wave velocity (UV) with yield stress (YS) and % of total change in ultrasonic velocity with % of total change in yield stress as compared to the service exposed (SE) condition.

Table 1 : % of total change in ultrasonic velocity and yield stress as compared to SE alloy for various precipitates and the values of slope (m) for precipitation and dissolution of various intermetallics phases.

Precipitate		Thermal treatment	Regions in Fig. 10		% of total change in ultrasonic velocity and yield stress as compared to SE alloy		Slope (m) of equation-5
			From condition	To condition	Ultrasonic velocity (% ΔV_x)	Yield strength (% ΔYS_x)	
Dissolution of $Ni_2(Cr, Mo)$		SE+923 K	O	A	-71	-33	3.8
γ"	Dissolution from SE alloy	-------	A	D	-29	-60	18.3
	Formation from RSA alloy	RSA+923 K	F	H	30	62	17.4
Dissolution of both $Ni_2(Cr, Mo)$ and γ"		SE+1123 K/1h	O	D	-100	-93	--
δ	Formation from SE alloy	SE+1123 K/ ≥10 h	D	E	-37	-20	4.5
	Formation from RSA alloy	RSA+1123 K	F	G	40	16	3.1
Dissolution of carbides		-------	D	F	0	7	--